

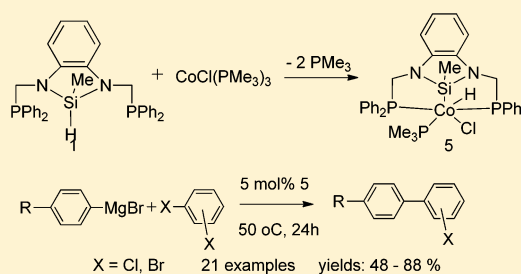
Synthesis and Reactivity of N-Heterocyclic PSiP Pincer Iron and Cobalt Complexes and Catalytic Application of Cobalt Hydride in Kumada Coupling Reactions

Zichang Xiong, Xiaoyan Li, Shumiao Zhang, Yaomin Shi, and Hongjian Sun*

School of Chemistry and Chemical Engineering, Key Laboratory of Special Functional Aggregated Materials, Ministry of Education, Shandong University, Shanda Nanlu 27, 250199 Jinan, People's Republic of China

Supporting Information

ABSTRACT: The new N-heterocyclic σ -silyl pincer ligand HSiMe-(NCH₂PPh₂)₂C₆H₄ (**1**) was designed. A series of tridentate silyl pincer Fe and Co complexes were prepared. Most of them were formed by chelate-assisted Si–H activation. The typical iron hydrido complex FeH(PMe₃)₂(SiMe(NCH₂PPh₂)₂C₆H₄) (**2**) was obtained by Si–H activation of compound **1** with Fe(PMe₃)₄. The combination of compound **1** with CoMe(PMe₃)₄ afforded the Co(I) complex Co(PMe₃)₂(SiMe(NCH₂PPh₂)₂C₆H₄) (**3**). The Co(III) complex CoHCl(PMe₃)₂(SiMe(NCH₂PPh₂)₂C₆H₄) (**5**) was generated by the reaction of complex **1** with CoCl(PMe₃)₃ or the combination of complex **3** with HCl. However, when complex **3** was treated with MeI, the Co(II) complex CoI(PMe₃)₂(SiMe(NCH₂PPh₂)₂C₆H₄) (**4**), rather than the Co(III) complex, was isolated. The catalytic performance of complex **5** for Kumada coupling reactions was explored. With a catalyst loading of 5 mol %, complex **5** displayed efficient catalytic activity for Kumada cross-coupling reactions of aryl chlorides and aryl bromides with Grignard reagents. This catalytic reaction mechanism is proposed and partially experimentally verified.



INTRODUCTION

In recent years, cyclometalated phosphine-based “PSiP” pincer complexes have enjoyed intense study,¹ especially tridentate silyl pincers of the type ((2-R’₂PC₆H₄)₂SiMeH, R’ = Ph, Cy, ^tBu, ⁱPr).² Researchers reported a series of tridentate silyl pincer complexes containing noble metals (Pd, Pt, Ir, etc.).^{2c,3} Most of these complexes are obtained by Si–H bond activation, and they have many applications. Iwasawa’s group used silyl pincer-type palladium complex to realize catalytic hydrocarboxylation of allenes with CO₂.⁴ In Shimada’s group, tridentate pincer-type bis(phosphino)silyl ligands (PSiP-R, R = Cy, ⁱPr, ^tBu) were used to synthesize the series of iridium tetrahydrido complexes [Ir(H)₄(PSiP-R)] under argon. When the same reaction was transferred to a nitrogen atmosphere, a rare example of a thermally stable iridium(III)–dinitrogen complex, [Ir(H)₂(N₂)(PSiP-R)], was isolated.⁵ Li’s group reported the novel cyclometalated iridium(III) complex [IrCl(H)(PSiP)] and this compound showed catalytic activity to the transfer hydrogenation of ketones to the corresponding secondary alcohols moderately with 2-propanol as the hydrogen source.^{2b} In the same year, Iwasawa’s group had developed an efficient method for the synthesis of various types of diborylalkenes from alkenes via a new PSiP-pincer palladium-catalyzed double dehydrogenative borylation.⁶ Our group has expended a great deal of effort in this field as well. In 2013, we reported the synthesis and characterization of a series of Ni, Co, and Fe complexes bearing a tridentate bis(phosphino)silyl ligand ((o-

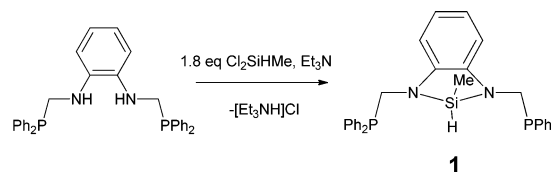
Ph₂PC₆H₄)₂SiMeH, [PSiP]-H). The hydrido iron(II) complex [PSiP]Fe(H)(PMe₃)₂ was found to be an excellent catalyst for the hydrosilylation of aldehydes and ketones under mild conditions.⁷ In 2015, we reported the synthesis and characterization of stable tripodal silyl iron and nickel complexes.⁸

Hill’s group designed the first example of N-heterocyclic σ -silyl pincer ligands bearing a PSiP-LXL donor triad.⁹ The noble metals Ru and Rh were used to form tridentate silyl pincer complexes via facile Si–H bond activation. On the basis of this, we designed the novel N-heterocyclic σ -silyl pincer ligand **1** and proved its good coordinating capability with non-noble metals. The catalytic ability of these chelate compounds was explored.

RESULTS AND DISCUSSION

Similar to the strategy by Hill,⁹ 1,3-siladiazoles HSiMe-(NCH₂PPh₂)₂C₆H₄ (**1**; Scheme 1) was synthesized by the

Scheme 1. Synthesis of Compound 1

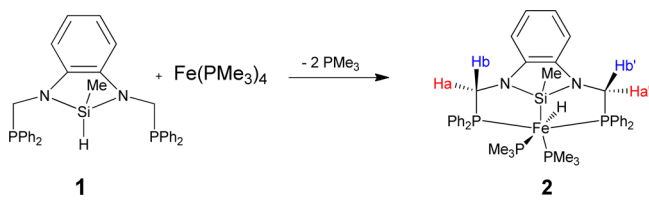


Received: November 10, 2015

reaction of $\text{C}_6\text{H}_4(\text{NHCH}_2\text{PPh}_2)_2$ with the chlorosilane MeHSiCl_2 in the presence of triethylamine in a yield of 75%. In the IR spectrum of **1**, the typical $\nu(\text{Si}-\text{H})$ stretching band is found at 2115 cm^{-1} . The characteristic Si-H signal is registered at 5.17 ppm as a multiplet in the ^1H NMR spectrum of **1**. In the ^{29}Si NMR spectrum of **1**, the characteristic silicon signal was found at -3.42 ppm as a doublet with the $^1\text{H}-^{29}\text{Si}$ coupling constant $J_{\text{HSi}} = 237\text{ Hz}$.

Reaction of $\text{Fe}(\text{PMe}_3)_4$ with $\text{HSiMe}(\text{NCH}_2\text{PPh}_2)_2\text{C}_6\text{H}_4$ (1**).** When compound **1** was treated with 1 equiv of $\text{Fe}(\text{PMe}_3)_4$ in THF (Scheme 2), the solution slowly turned dark red-

Scheme 2. Synthesis of Complex **2**



brown. After 14 h, complex **2** was isolated as orange bulk crystals from diethyl ether. In the IR spectrum of **2**, the typical $\nu(\text{Fe}-\text{H})$ stretching band of complex **2** is found at 1840 cm^{-1} . In the ^1H NMR spectrum of **2**, the characteristic iron hydrido

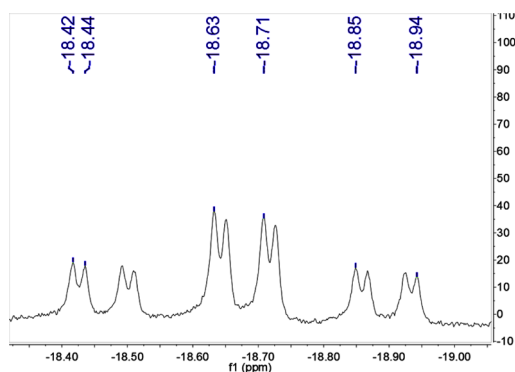


Figure 1. Hydrido resonance of complex **2**.

signal (Figure 1) is found at -18.70 ppm as a tdd peak with the $^{31}\text{P}-^1\text{H}$ coupling constants $J_{\text{PH}} = 66, 24, 6\text{ Hz}$. The resonance is first split into a triplet by the two phosphorus atoms of the PPh_2 groups. Then, each phosphorus atom of the PMe_3 group splits the triplet into a doublet of doublets. In preligand **1**, the four methylene hydrogen atoms have the same chemical environment; therefore, they cannot be distinguished by ^1H NMR spectroscopy. In complex **2**, the four methylene hydrogen atoms have different chemical environments due to the formation of the structure of complex **2**. Even the two hydrogen atoms of the same methylene group can be also distinguished by ^1H NMR spectroscopy. For example, the Ha atom is coupled with Hb and then further coupled with the nearby phosphorus atom to split into a pseudotriplet (Scheme 2 and Figure 2). However, the chemical shifts of Ha and Ha' are very close and much different from those of Hb and Hb'. This result is further proved by ^{13}C NMR spectroscopy. Two methylene carbon atoms were recorded at 63.86 and 64.02 ppm. This phenomenon can be explained by the fixation of the two methylene groups caused by the coordination of the preligand.

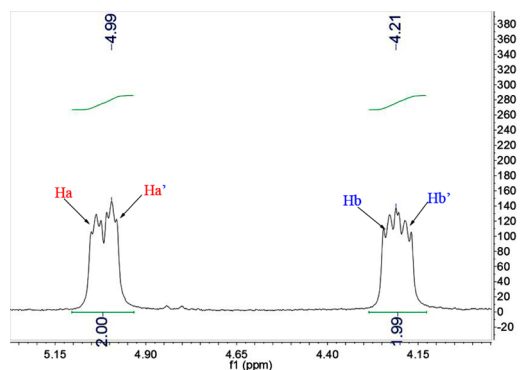


Figure 2. ^1H NMR of PCHaHbN and PCHa'Hb'N of complex **2**.

X-ray crystallography was used to confirm the structure of complex **2** (Figure 3). The structure of complex **2** is a distorted

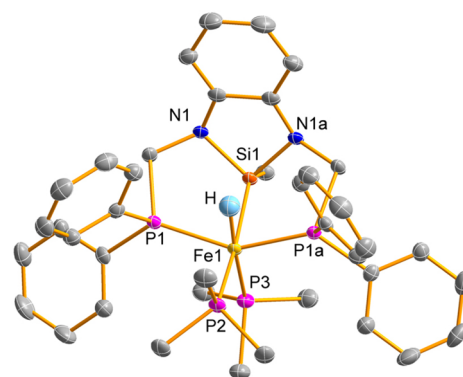


Figure 3. ORTEP plot of complex **2** at the 50% probability level (most of the hydrogen atoms are omitted for clarity). Selected bond lengths (Å) and angles (deg): $\text{Fe1}-\text{P1}$ 2.2095(6), $\text{Fe1}-\text{P1a}$ 2.2095(6), $\text{Fe1}-\text{P2}$ 2.2742(9), $\text{Fe1}-\text{P3}$ 2.226(1), $\text{Fe1}-\text{Si1}$ 2.2643(9), $\text{Fe1}-\text{H}$ 1.47(3); $\text{P1}-\text{Fe1}-\text{H}$ 74.66(2), $\text{P1}-\text{Fe1}-\text{P3}$ 104.05(2), $\text{Si1}-\text{Fe1}-\text{P2}$ 166.30(4).

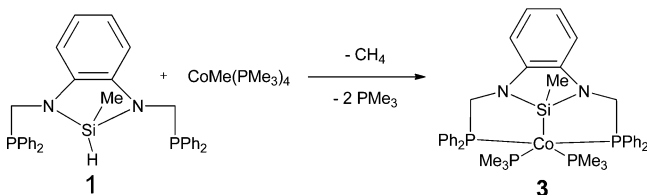
hexacoordinate octahedral structure. The axial angle $\text{P2}-\text{Fe1}-\text{Si1}$ is 166.30° , deviating from 180° . The sum of equatorial plane bond angles is 357.41° , deviating from 360° . Due to the strong trans influence of Si and H atoms, $\text{Fe1}-\text{P2}$ (2.2742(9) Å) and $\text{Fe1}-\text{P3}$ (2.226(1) Å) are remarkably longer than $\text{Fe1}-\text{P1}$ (2.2095(6) Å) and $\text{Fe1}-\text{P1a}$ (2.2095(9) Å). The $\text{Fe1}-\text{H}$ bond (1.47 Å) is in the normal scope of an $\text{Fe}-\text{H}$ bond.¹⁰ The whole molecule has the symmetry plane $[\text{Si1P3P2H}]$. Complex **2** belongs to point group Cs .

Recently, several hydrido iron pincer complexes have been reported as catalysts for the reduction of unsaturated compounds.¹¹ In addition, our group has reported iron hydrido complexes for the reduction of aldehydes and ketones.^{7,12} These all proved that hydrido iron pincer complexes are potential effective catalysts. Therefore, the catalytic activity of complex **2** was tested for the reduction of aldehydes. Several aldehydes were chosen as substrates with $(\text{EtO})_3\text{SiH}$ as a hydrogen source. The reactions were carried out with 30 mol % catalyst and a reaction temperature of $60-80^\circ\text{C}$. Unfortunately, low conversions of substrates were found (determined by GC). The result might be because the large electronegativity of nitrogen atoms makes the silicon atom become a better π acceptor. This structure makes the metal center more stable. Therefore, the PMe_3 ligand cannot easily dissociate from the

iron center and there is no coordination vacancy for the catalytic reaction.

Reaction of $\text{CoMe}(\text{PMe}_3)_4$ with $\text{HSiMe}(\text{NCH}_2\text{PPh}_2)_2\text{C}_6\text{H}_4$ (1). Compound 1 in 40 mL of THF was combined with $\text{CoMe}(\text{PMe}_3)_4$ in 20 mL of THF (Scheme 3);

Scheme 3. Synthesis of Complex 3



the solution turned dark red from bright transparent red after being stirred for 48 h. Complex 3 was isolated as red crystals from a mixed solvent (diethyl ether/pentane, 1/1). The PMe_3 signals of complex 3 in the ^1H NMR spectrum (δ 0.82 and 1.29 ppm) and in the ^{31}P NMR spectrum (δ -2.42 and 16.89 ppm) clearly indicate that the two trimethylphosphine ligands are not in the same chemical environment. X-ray crystallography data indicate that the structure of 3 has a trigonal-bipyramidal coordination geometry (Figure 4). [P2P3P4] is the equatorial

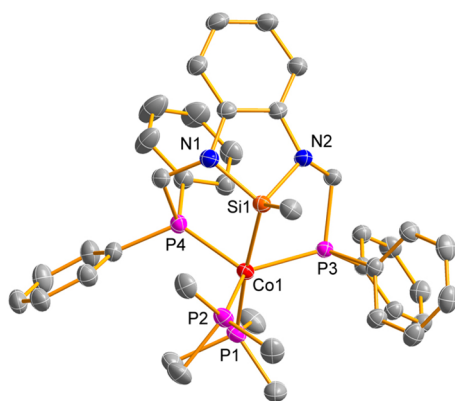


Figure 4. ORTEP plot of complex 3 at the 50% probability level (hydrogen atoms are omitted for clarity). Selected bond lengths (Å) and angles (deg): Co1–P4 2.1820(5), Co1–P3 2.1885(5), Co1–P2 2.1964(5), Co1–P1 2.2148(5), Co1–Si1 2.2559(5), Co2–P8 2.1817(5), Co2–P7 2.1958(5), Co2–P5 2.2180(5), Co2–P6 2.2232(5), Co2–Si2 2.2748(5); P4–Co1–P3 122.67(2), P4–Co1–P2 106.84(2), P3–Co1–P2 124.97(2), P4–Co1–P1 99.22(2), P3–Co1–P1 96.99(2), P2–Co1–P1 7.31(2), P1–Co1–Si1 172.79(2).

plane, and the Si1–Co1–P1 group is in the axial position. This is accompanied by some distortions from ideality. The axial angle of P1–Co1–Si1 is $172.79(2)^\circ$, deviating from 180° . The sum of the equatorial plane bond angles is 354.48° , deviating from 360° . The Co–P bonds of complex 3 are shorter than usual Co–P bonds.¹³

Reaction of MeI with $\text{Co}(\text{PMe}_3)_2(\text{SiMe}(\text{NCH}_2\text{PPh}_2)_2\text{C}_6\text{H}_4)$ (3). Complex 3 was treated with CH_3I in THF (Scheme 4). The solution turned dark brown quickly from red. Finally, complex 4 was isolated as orange crystals from a mixed solvent (THF/pentane, 1/1). Cobalt(II) complex 4 is paramagnetic. The crystal data of complex 4 indicate that it has a trigonal-bipyramidal coordination geometry (Figure 5). [P1P2I1] is the equatorial plane, and the Si1–Co1–P3 group is in the axial position. The P3–Co1–Si1 axial bond angle is

Scheme 4. Synthesis of Complex 4

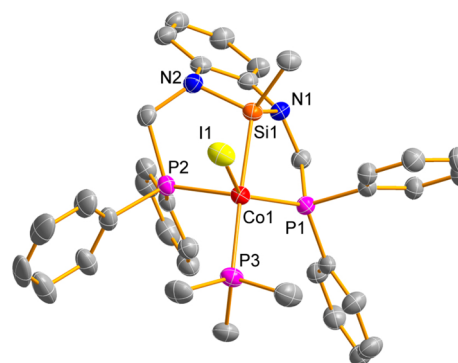
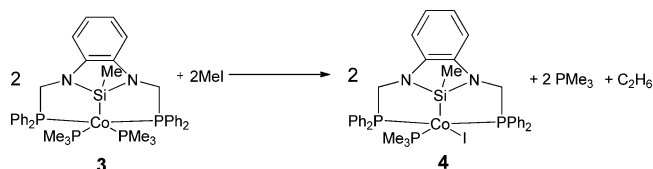
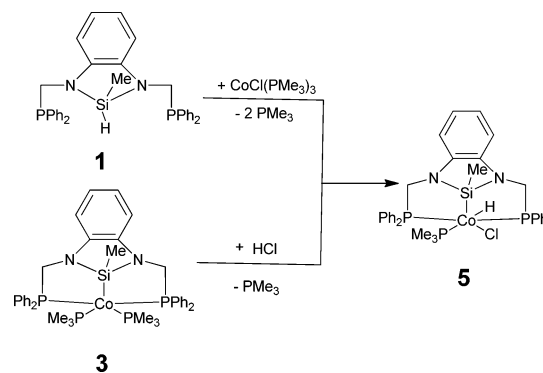


Figure 5. ORTEP plot of complex 4 at the 50% probability level (hydrogen atoms are omitted for clarity). Selected bond lengths (Å) and angles (deg): I1–Co1 2.6099(5), Co1–P1 2.208(1), Co1–P2 2.235(1), Co1–P3 2.265(1), Co1–Si1 2.280(1); P1–Co1–P2 110.19(4), P3–Co1–Si1 176.01(4), P1–Co1–I1 139.44(3), P2–Co1–I1 104.09(3).

176.01° , deviating from 180° , and the sum of equatorial plane bond angles is 353.72° , deviating from 360° . The Co–P bonds of complex 4 are longer than those of complex 3. The Co–Si bond (2.28 Å) of complex 4 is particularly long in this series of cobalt complexes. It is conjectured that the process from 3 to 4 is a radical mechanism. The addition of iodo radical, formed via homolytic cleavage of iodomethane, to the cobalt(I) center of 3 gives rise to the cobalt(II) center of 4. Two methyl radicals form one molecule of ethane. The formation of ethane was confirmed by an in situ ^1H NMR spectrum with a chemical shift of 0.89 ppm.⁷ In this process the pentacoordinate 18-electron cobalt(I) complex 3 transforms to the pentacoordinate 17-electron cobalt(II) species 4.

Synthesis of $\text{CoHCl}(\text{PMe}_3)_3(\text{SiMe}(\text{NCH}_2\text{PPh}_2)_2\text{C}_6\text{H}_4)$ (5). In our early work, $\text{CoCl}(\text{PMe}_3)_3$ was proven to be an effective Si–H activation reagent.^{7,8} Thus, compound 1 and $\text{CoCl}(\text{PMe}_3)_3$ were combined in THF (Scheme 5). After the mixture was stirred for 20 h, hydrido cobalt(III) complex 5 as a Si–H activation product was isolated from diethyl ether. Complex 5

Scheme 5. Different Strategies for Preparing Complex 5



can also be prepared by combining complex **3** with HCl in THF. The typical $\nu(\text{Co-H})$ stretching band is found at 1985 cm^{-1} in the IR spectrum of **5**. In the ^1H NMR of **5**, the resonance of the hydrido hydrogen is at -28.78 ppm (Figure 6). It is split into a quartet because the hydrogen atom is

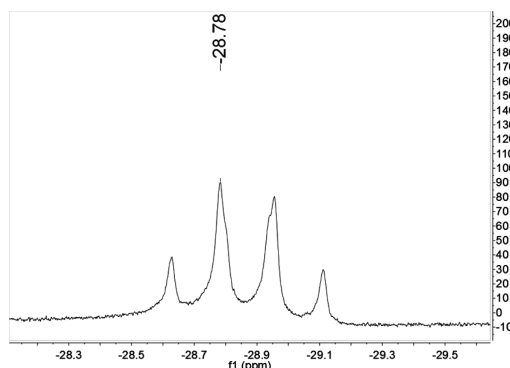


Figure 6. Hydrido resonance of complex **5**.

coupled with three phosphorus atoms in PPh_2 and PMe_3 . Similar to the case for complex **2**, the two hydrogen atoms in the methylene group of complex **5** also lie in different chemical environments. However, the difference between two chemical shifts is smaller than that of complex **2**. X-ray crystallography data indicate that the structure of **5** features octahedral coordination (Figure 7). $[\text{P1P3Si1P2}]$ is the equatorial plane,

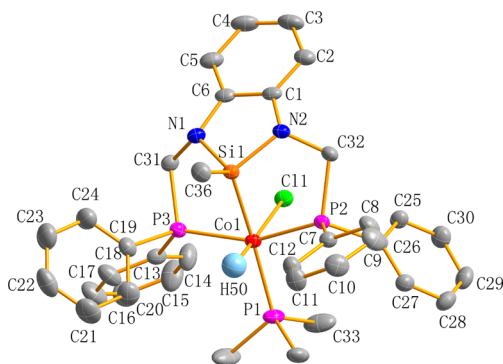


Figure 7. ORTEP plot of complex **5** at the 50% probability level (most hydrogen atoms are omitted for clarity). Selected bond lengths (Å) and angles (deg): Co1–P1 2.2364(5), Co1–P2 2.2063(4), C1–P3 2.1976(4), Co1–Si1 2.2480(5), Co1–Cl1 2.3316(4), Co1–H50 1.38(2); Cl1–Co1–H50 178.8(1), P2–Co1–Si1 78.909(2), P3–Co1–Si1 78.079(2), P1–Co1–P3 105.438(2), P1–Co1–P2 97.957(2).

and the Cl1–Co1–H50 group is in the axial position. This is accompanied by some distortions from ideality as well. The axial bond angle of Cl1–Co1–H50 is 178.8° , slightly deviating from 180° . The sum of equatorial plane bond angles is 360.38° , very close to 360° . In addition, because of the strong trans influence of Si, the Co1–P1 bond (2.2364(5) Å) is longer than both Co1–P2 (2.2063(4) Å) and Co1–P3 (2.1976(4) Å) bonds.

Catalytic Application of Complex 5 in Kumada Coupling Reactions. Complex **5** is a Co(III) compound containing a Co–H and a Co–Cl together. This structure was assumed to be an unstable structure sometimes,¹⁴ making the complex a potential catalyst. Early work demonstrated that

some complexes containing Co–Cl bond can catalyze Kumada coupling reactions.¹⁵ Encouraged by these results, we studied a series of Kumada coupling reactions catalyzed by complex **5**.

At the beginning, the Kumada cross-coupling of chlorobenzene with (4-methylphenyl)magnesium bromide catalyzed by complex **5** was used as a probe reaction. When the temperature was below 60°C , there was little homocoupling product of the Grignard reagent. However, when the temperature was increased to 60°C , the homocoupling product of the Grignard reagent was obviously formed according to GC analysis. When the temperature was increased to 80°C with dioxane as solvent, the conversion declined sharply. A gray precipitate appeared in the solution. The catalyst should have decomposed. Finally, the reaction conditions 50°C , 48 h, and THF as the solvent (Table 1, entry 4) were adopted.

Table 1. Kumada Cross-Coupling Reactions of Chlorobenzene with (4-Methylphenyl)magnesium Bromide Catalyzed by **5**

entry	time (h)	temp ($^\circ\text{C}$)	solvent	conversion (%)
1	24	25	THF	30
2	48	25	THF	60
3	48	40	THF	75
4	48	50	THF	90
5	48	50	toluene	60
6	48	60	THF	85
7	48	80	dioxane	<10

Under the optimized conditions, a series of reactions of 4- R_1 -chlorobenzene with (4- R_2 -phenyl)magnesium bromide were examined (Table 2). It can be summarized from Table 2 that

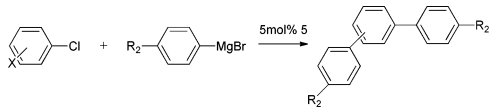
Table 2. Kumada Cross-Coupling Reactions of Aryl Chlorides with Grignard Reagents Catalyzed by **5**^a

entry	R_1	R_2	yield ^b (%)
1	H	Me	84
2	H	OMe	70
3	Me	H	80
4	Me	OMe	72
5	OMe	H	65
6	OMe	Me	67

^aConditions: 50°C , 48 h. ^bIsolated yields.

aryl chlorides with an H or Me group give higher yields than aryl chlorides with an OMe group. These reactions prove that complex **5** is an effective catalyst for Kumada cross-coupling reactions. In Table 3, we examined cross-coupling reactions of dihalogenated phenyl with (4- R_2 -phenyl)magnesium bromide. The yields of these reactions are relatively lower than those for monosubstituted Kumada coupling reactions. From entries 1 and 2, it could be seen that, due to the potential steric hindrance effect, lower yields were obtained for *o*-dichlorobenzene as the substrate in comparison to those for *m*-dichlorobenzene and *p*-dichlorobenzene.

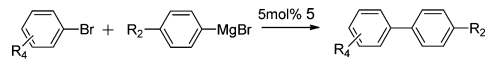
At the same time, a series of Kumada cross-coupling reactions of different aryl bromides with Grignard reagents

Table 3. Kumada Cross-Coupling Reactions of Aryl Dichlorides with Grignard Reagents Catalyzed by **5**^a


entry	X	R ₂	yield ^b (%)
1	<i>o</i> -Cl	H	56
2	<i>o</i> -Cl	Me	48
3	<i>m</i> -Cl	H	68
4	<i>m</i> -Cl	Me	72
5	<i>p</i> -Cl	H	75
6	<i>p</i> -Cl	Me	65

^aConditions: 50 °C, 48 h. ^bIsolated yields.

catalyzed by complex **5** were explored. The reaction temperature was 10 °C, lower than that for the aforementioned reactions. The reaction time was shortened to half of the time used for the above reactions. From Table 4, it is concluded that

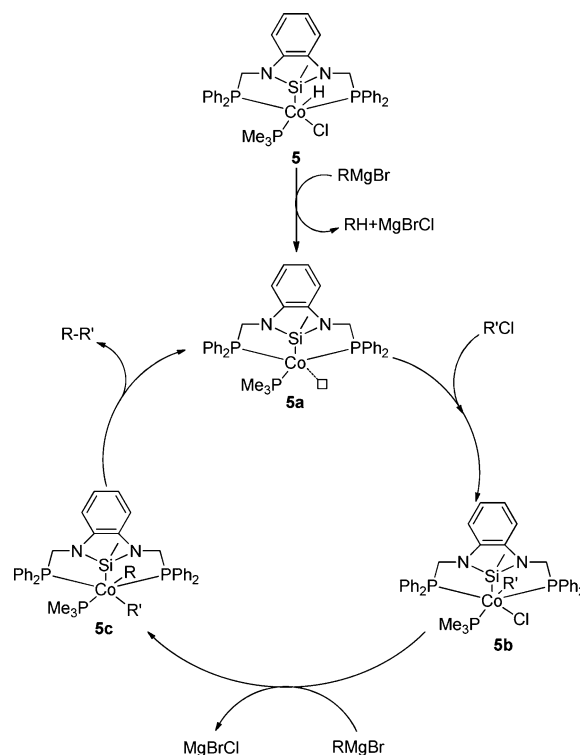
Table 4. Kumada Cross-Coupling Reactions of Aryl Bromides with Grignard Reagents Catalyzed by Complex **5**^a


entry	R ₄	R ₂	yield ^b (%)
1	H	Me	88
2	H	OMe	75
3	<i>p</i> -Me	H	85
4	<i>p</i> -Me	OMe	82
5	<i>p</i> -OMe	H	78
6	<i>p</i> -OMe	Me	85
7	<i>o</i> -Me	H	83
8	<i>o</i> -Me	Me	80
9	<i>o</i> -Me	OMe	70

^aConditions: 40 °C, 24 h. ^bIsolated yields.

complex **5** showed better catalytic activity for Kumada cross-coupling reaction of aryl bromides with Grignard reagents. Through literature retrieval, we found that it is the first hydrido cobalt(III) chloride catalyst for Kumada cross-coupling reactions.

On the basis of related literatures,¹⁶ the reaction mechanism is hypothesized (Scheme 6). At first, complex **5** reacts with Grignard reagent to form intermediate **5a** with one vacant coordination site. Then oxidative addition of R'Cl to intermediate **5a** gives rise to intermediate **5b**, followed by transmetalation of RMgBr to form intermediate **5c**. Finally, reductive elimination of intermediate **5c** leads to formation of R-R' with the recovery of intermediate **5a**. In order to verify the reaction mechanism proposed in Scheme 6, the following three experiments were designed. A stoichiometric reaction between complex **5** and (4-methylphenyl)magnesium bromide was carried out in THF. The reaction solution was placed at 50 °C for 24 h. This solution turned red from dark yellow. Before further operation, GC-MS measurements were used to analyze the solution. Toluene was detected (page S20 in the Supporting Information). After that, volatiles were removed in vacuo. Diethyl ether and *n*-pentane were used to extract the solid. However, attempts to isolate intermediate **5a** failed. Perhaps **5a** as an unstable intermediate decomposed to the unknown gray white solid. In the process of isolating and confirming the

Scheme 6. Proposed Mechanism for Complex **5** Catalyzed Kumada Coupling Reactions

intermediate **5a**, another stoichiometric reaction between complex **5** and (4-methylphenyl)magnesium bromide was carried out in THF again in the presence of 1 equiv of trimethylphosphine as a supporting ligand. The reaction solution was heated to 50 °C for 24 h. Finally, complex **3** was isolated from *n*-pentane. This gave evidence for the presence of **5a**. A stoichiometric reaction between complex **5** and chlorobenzene was also operated. However, these two substances did not react with each other.

CONCLUSION

The new silyl pincer proligand HSiMe(NCH₂PPh₂)₂C₆H₄ (**1**) is designed. A series of studies of the reactions of complex **1** with electron-rich iron and cobalt complexes supported by trimethylphosphine ligands were carried out. Novel tridentate silyl pincer Fe and Co complexes **2**–**5** were prepared via Si–H bond activation. With a catalyst loading of 5 mol %, complex **5** displays efficient catalytic activity for Kumada cross-coupling reactions of aryl chlorides and aryl bromides with Grignard reagents. A catalytic reaction mechanism was proposed and partially experimentally verified.

EXPERIMENTAL SECTION

General Procedures and Materials. All air-sensitive materials were prepared and used under a nitrogen atmosphere with the standard Schlenk techniques. *n*-Pentane, diethyl ether, THF, and toluene were dried by distillation from Na–benzophenone under nitrogen before use. Fe(PMe₃)₄,¹⁷ CoMe(PMe₃)₄,¹⁸ and CoCl(PMe₃)₃¹⁹ were prepared by the literature methods. The Grignard reagents were prepared from the corresponding bromide and magnesium turnings in anhydrous tetrahydrofuran (THF) according to the known procedures²⁰ and were titrated prior to use. All other chemicals were purchased and used as received without further purification. Infrared spectra (4000–400 cm^{−1}), as obtained from Nujol mulls between KBr disks, were recorded on a Bruker ALPHA

FT-IR instrument. ^1H , $^{13}\text{C}\{^1\text{H}\}$, $^{29}\text{Si}\{^1\text{H}\}$, and $^{31}\text{P}\{^1\text{H}\}$ NMR spectra (300, 75, 60, and 121 MHz, respectively) were recorded on a Bruker Avance 300 spectrometer with C_6D_6 as the solvent without an internal reference at room temperature. Elemental analyses were carried out on an Elementar Vario ELIII instrument.

Synthesis of $\text{HSiMe}(\text{NCH}_2\text{PPh}_2)_2\text{C}_6\text{H}_4$ (1). Triethylamine (2.93 g, 29.00 mmol) was added to a stirred solution of $\text{C}_6\text{H}_4(\text{NHCH}_2\text{PPh}_2)_2$ (7.3 g, 14.48 mmol) in THF (100 mL). Dichloromethylsilane (3.0 g, 26.09 mmol) was added dropwise to the stirred solution. The resultant suspension was stirred for 2 days and then stored at 4 °C for 2 h. The supernatant was isolated by filtration, and volatiles were removed in vacuo, leaving a sticky solid. This was extracted with benzene, and the residual precipitate was removed by filtration. The benzene was removed in vacuo; then trituration of the solid in pentane/diethyl ether (1/1, 50 mL) yielded a white precipitate, which was isolated by cannula filtration. Yield: 74.8%. IR (Nujol, KBr, cm^{-1}): 3050 (Ar–H), 2116 (Si–H). ^1H NMR (300 MHz, CDCl_3 , δ/ppm): 0.12 (m, 3H, CH_3), 3.94 (m, 4H, CH_2), 5.17 (m, 1H, SiH), 6.74 (s, 4H, C_6H_4), 7.33–7.48 (m, 20H, C_6H_5). ^{31}P NMR (121 MHz, CDCl_3 , δ/ppm): –22.99 (s, P, PPh_2). ^{13}C NMR (75 MHz, CDCl_3 , δ/ppm): 0.00 (t, SiCH_3), 44.02 (d, CH_2), 106.08 (d, Ar), 127.00 (dd, Ar), 127.51 (d, Ar), 131.11–131.64 (m, Ar), 135.31–135.85 (m, Ar), 139.24 (d, Ar). ^{29}Si NMR (79.45 MHz, CDCl_3 , δ/ppm): –3.42 (d, $J = 237$ Hz). Anal. Calcd for $\text{C}_{33}\text{H}_{32}\text{N}_2\text{P}_2\text{Si}$ (546.18 g/mol): C, 72.51; H, 5.90; N, 5.12. Found: C, 72.70; H, 5.72; N, 5.34.

Synthesis of $\text{FeH}(\text{PMe}_3)_2(\text{SiMe}(\text{NCH}_2\text{PPh}_2)_2\text{C}_6\text{H}_4)$ (2). Compound 1 (0.8 g, 1.46 mmol) in 40 mL of THF was treated with $\text{Fe}(\text{PMe}_3)_4$ (0.55 g, 1.53 mmol) in 20 mL of THF with stirring at room temperature for 24 h. After removal of the volatiles under reduced pressure, the residue was extracted with pentane and diethyl ether. Compound 2 (0.74 g, 0.98 mmol) was isolated as yellow crystals in 67% yield from diethyl ether at room temperature. IR (Nujol, KBr, cm^{-1}): 3050 (Ar–H), 1840 (Fe–H), 937 (PMe_3). ^1H NMR (300 MHz, C_6D_6 , δ/ppm): –18.6 (tdd, $J = 66, 24, 6$ Hz, 1H, Fe–H), 0.60 (d, 9H, PMe_3), 0.87 (s, 3H, SiCH_3), 1.28 (d, 9H, PMe_3), 4.21 (m, 2H, PCHaHbN), 4.99 (m, 2H, PCHa'Hb'N), 6.82–7.31 (m, 20H, C_6H_5), 7.84 (s, 4H, C_6H_4). ^{31}P NMR (121 MHz, C_6D_6 , δ/ppm): 17.42 (m, 1P, PMe_3), 21.47 (m, 1P, PMe_3), 110.26 (m, 2P, PPh_2). ^{13}C NMR (75 MHz, C_6D_6 , δ/ppm): 12.88 (d, SiCH_3), 25.08 (d, PCH_3), 28.16 (d, PCH_3), 63.85 (m, CH_2), 64.02 (m, CH_2), 112.78 (Ar), 117.96 (Ar), 129.48 (Ar), 132.55 (Ar), 135.54 (Ar), 140.90 (Ar), 145.87 (Ar), 149.49 (Ar). Anal. Calcd for $\text{C}_{39}\text{H}_{50}\text{FeN}_2\text{P}_4\text{Si}$ (754.63 g/mol): C, 62.07; H, 6.68; N, 3.71. Found: C, 61.99; H, 6.48; N, 3.68.

Synthesis of $\text{Co}(\text{PMe}_3)_2(\text{SiMe}(\text{NCH}_2\text{PPh}_2)_2\text{C}_6\text{H}_4)$ (3). Compound 1 (0.53 g, 0.97 mmol) in 40 mL of THF was combined with $\text{CoMe}(\text{PMe}_3)_4$ (0.38 g, 1.02 mmol) in 20 mL of THF with stirring at room temperature for 48 h. After removal of the volatiles under reduced pressure the residue was extracted with pentane and mixed solvent (diethyl ether/pentane, 1/1). Compound 3 (0.53 g, 0.70 mmol) was isolated as red crystals in 72% yield from mixed solvent (diethyl ether/pentane, 1/1) at 0 °C. ^1H NMR (300 MHz, C_6D_6 , δ/ppm): 0.65 (s, 3H, SiCH_3), 0.82 (d, $J = 6.3$ Hz, 9H, PCH_3), 1.29 (d, $J = 5.4$ Hz, 9H, PCH_3), 4.24 (m, 4H, CH_2), 6.93–7.41 (m, 20H, C_6H_5), 7.79 (s, 4H, C_6H_4). ^{31}P NMR (121 MHz, C_6D_6 , δ/ppm): –2.42 (m, 1P, PMe_3), 16.89 (m, 1P, PMe_3), 77.48 (m, 2P, PPh_2). ^{13}C NMR (75 MHz, C_6D_6 , δ/ppm): 12.26 (m, SiCH_3), 24.09 (d, PCH_3), 26.94 (d, PCH_3), 61.97 (m, CH_2), 114.90 (Ar), 119.87 (Ar), 132.97 (Ar), 142.39 (Ar), 148.37 (Ar). Anal. Calcd for $\text{C}_{39}\text{H}_{49}\text{CoN}_2\text{P}_4\text{Si}$ (756.70 g/mol): C, 61.90; H, 6.53; N, 3.70. Found: C, 62.13; H, 6.80; N, 3.92.

Synthesis of $\text{CoIPMe}_3\text{SiMe}(\text{NCH}_2\text{PPh}_2)_2\text{C}_6\text{H}_4$ (4). Complex 3 (0.62 g, 0.82 mmol) in 40 mL of THF was treated with MeI (0.12 g, 0.82 mmol) in 20 mL of THF with stirring at room temperature for 24 h. After removal of the volatiles under reduced pressure the residue was extracted with pentane and THF/diethyl ether. Compound 4 (0.50 g, 0.62 mmol) was isolated as dark yellow crystals in 68% yield from THF/diethyl ether at –30 °C. IR (Nujol, KBr, cm^{-1}): 3057 (Ar–H), 950 (PMe_3). Anal. Calcd for $\text{C}_{36}\text{H}_{40}\text{CoIN}_2\text{P}_3\text{Si}$ (807.53 g/mol): C, 53.54; H, 4.99; N, 3.47. Found: C, 53.35; H, 5.18; N, 3.60.

Synthesis of $\text{CoHCIPMe}_3\text{SiMe}(\text{NCH}_2\text{PPh}_2)_2\text{C}_6\text{H}_4$ (5). (a) A mixture of complex 1 (0.47 g, 0.86 mmol) and $\text{CoCl}(\text{PMe}_3)_3$ (0.30

g, 0.95 mmol) was dissolved in 60 mL of THF. The resultant mixture was stirred at room temperature for 24 h. After removal of the volatiles under reduced pressure the residue was extracted with pentane and diethyl ether. Compound 5 (0.49 g, 0.69 mmol) was isolated as yellow crystals in 80% yield from diethyl ether at room temperature.

(b) HCl (0.59 mL, 1.26 mol/L in Et_2O) was added to complex 3 (0.57 g, 0.75 mmol) in 40 mL of THF with stirring at room temperature for 12 h. After removal of the volatiles under reduced pressure the residue was extracted with pentane and diethyl ether. Compound 5 (0.32 g, 0.45 mmol) was isolated as yellow crystals in 60% yield from diethyl ether at room temperature. IR (Nujol, KBr, cm^{-1}): 3050 (Ar–H), 1985 (Co–H), 937 (PMe_3). ^1H NMR (300 MHz, C_6D_6 , δ/ppm): –28.78 (q, $J = 45$ Hz, 1H, Co–H), 0.00 (s, 3H, SiCH_3), 0.97 (d, $J = 7.2$ Hz, 9H, PCH_3), 4.65–4.77 (m, 4H, CH_2), 7.08–7.34 (m, 20H, C_6H_5), 8.02 (m, 4H, C_6H_4). ^{31}P NMR (121 MHz, C_6D_6 , δ/ppm): 5.18 (s, 1P, PMe_3), 84.39 (s, 2P, PPh_2). ^{13}C NMR (75 MHz, C_6D_6 , δ/ppm): 10.64 (d, SiCH_3), 19.45 (m, PCH_3), 57.31 (m, CH_2), 112.93 (Ar), 119.78 (Ar), 129.69 (Ar), 133.43 (Ar), 134.53 (Ar), 149.90 (Ar). Anal. Calcd for $\text{C}_{36}\text{H}_{41}\text{ClCoN}_2\text{P}_3\text{Si}$ (717.09 g/mol): C, 60.29; H, 5.76; N, 3.91. Found: C, 60.43; H, 5.78; N, 3.87.

X-ray Structure Determination. Diffraction data were collected on a Bruker SMART Apex II CCD diffractometer equipped with graphite-monochromated Mo $K\alpha$ radiation ($\lambda = 0.71073$ Å). The structures were resolved by direct or Patterson methods with the SHELXS-97 program and were refined on F^2 with SHELXTL. Hydrogen atoms were included in calculated positions and were refined using a riding model. A summary of crystal data, data collection parameters, and structure refinement details is given in the Supporting Information. CCDC-1427407 (2), CCDC-1427422 (3), CCDC-1427421 (4), and CCDC-1427423 (5) contain supplementary crystallographic data for this paper. Copies of the data can be obtained free of charge on application to the CCDC, 12 Union Road, Cambridge CB2 1EZ, U.K. (fax, (+44)1223-336-033; e-mail, deposit@ccdc.cam.ac.uk).

Representative Experimental Procedure for Cross-Coupling Reaction. Under a N_2 atmosphere complex 5 (2 mL, 0.025 mmol/mL in THF) was placed in a Schlenk tube. Chlorobenzene (0.106 g, 1 mmol) and (4-methylphenyl)magnesium bromide (1 mL, 1.22 mmol/mL in THF) were added. The reaction mixture was stirred for 48 h at 50 °C and was quenched with 10 mL of H_2O . The product was extracted three times with 50 mL of Et_2O . The organic layers were combined and dried over Na_2SO_4 . All volatiles were removed under reduced pressure. The crude product was purified by column chromatography over silica gel with petroleum ether as eluent to provide the corresponding product.

■ ASSOCIATED CONTENT

§ Supporting Information

The Supporting Information is available free of charge on the ACS Publications website at DOI: [10.1021/acs.organomet.5b00937](https://doi.org/10.1021/acs.organomet.5b00937).

Crystallographic data for 2–5 and the original IR, ^1H NMR, ^{31}P NMR, ^{13}C NMR, and ^{29}Si NMR spectra of the complexes (PDF)

Crystallographic data for 2–5 (CIF)

■ AUTHOR INFORMATION

Corresponding Author

*E-mail for H.S.: hjsun@sdu.edu.cn.

Notes

The authors declare no competing financial interest.

■ ACKNOWLEDGMENTS

We gratefully acknowledge financial support by NSF China No. 21272138/21572119 and support from Prof. Dr. Dieter Fenske

and Dr. Olaf Fuhr (Karlsruhe Nano-Micro Facility) in the determination of the crystal structures.

■ REFERENCES

- (1) (a) Tsay, C.; Mankad, N. P.; Peters, J. C. *J. Am. Chem. Soc.* **2010**, *132*, 13975–13977. (b) Takaya, J.; Iwasawa, N. *Organometallics* **2009**, *28*, 6636–6638. (c) Mitton, S. J.; McDonald, R.; Turculet, L. *Angew. Chem., Int. Ed.* **2009**, *48*, 8568–8571.
- (2) (a) MacInnis, M. C.; MacLean, D. F.; Lundgren, R. J.; McDonald, R.; Turculet, L. *Organometallics* **2007**, *26*, 6522–6525. (b) Li, Y. H.; Zhang, Y.; Ding, X. H. *Inorg. Chem. Commun.* **2011**, *14*, 1306–1310. (c) Takaya, J.; Iwasawa, N. *Dalton Trans.* **2011**, *40*, 8814–8821.
- (3) Suh, H.-W.; Guard, L. M.; Hazari, N. *Chem. Sci.* **2014**, *5*, 3859–3872.
- (4) Takaya, J.; Iwasawa, N. *J. Am. Chem. Soc.* **2008**, *130*, 15254–15255.
- (5) Fang, H. Y.; Choe, Y. K.; Li, Y. H.; Shimada, S. *Chem. - Asian J.* **2011**, *6*, 2512–2521.
- (6) Takaya, J.; Kirai, N.; Iwasawa, N. *J. Am. Chem. Soc.* **2011**, *133*, 12980–12983.
- (7) Wu, S. Q.; Li, X. Y.; Xiong, Z. C.; Xu, W. G.; Lu, Y. Q.; Sun, H. J. *Organometallics* **2013**, *32*, 3227–3237.
- (8) Xu, S. L.; Li, X. Y.; Zhang, S. M.; Sun, H. J. *Inorg. Chim. Acta* **2015**, *430*, 161–167.
- (9) Dixon, L. S. H.; Hill, A. F.; Sinha, A.; Ward, J. S. *Organometallics* **2014**, *33*, 653–658.
- (10) Bhattacharya, P.; Krause, J. A.; Guan, H. *Organometallics* **2011**, *30*, 4720–4729.
- (11) (a) Werkmeister, S.; Junge, K.; Wendt, B.; Alberico, E.; Jiao, H.; Baumann, W.; Junge, H.; Gallou, F.; Beller, M. *Angew. Chem., Int. Ed.* **2014**, *53*, 8722–8726. (b) Zell, T.; Ben-David, Y.; Milstein, D. *Angew. Chem., Int. Ed.* **2014**, *53*, 4685–4689. (c) Chakraborty, S.; Dai, H.; Bhattacharya, P.; Fairweather, N. T.; Gibson, M. S.; Krause, J. A.; Guan, H. *J. Am. Chem. Soc.* **2014**, *136*, 7869–7872. (d) Bhattacharya, P.; Krause, J. A.; Guan, H. *J. Am. Chem. Soc.* **2014**, *136*, 11153–11161.
- (12) (a) Zuo, Z. Y.; Sun, H. J.; Wang, L.; Li, X. Y. *Dalton Trans.* **2014**, *43*, 11716–11722. (b) Zhao, H.; Sun, H. J.; Li, X. Y. *Organometallics* **2014**, *33*, 3535–3539. (c) Xue, B. J.; Sun, H. J.; Li, X. Y. *RSC Adv.* **2015**, *5*, 52000–52006.
- (13) (a) Li, J. Y.; Zheng, T. T.; Sun, H. J.; Xu, W. G.; Li, X. Y. *Dalton Trans.* **2013**, *42*, 5740–5748. (b) Zheng, T. T.; Sun, H. J.; Lu, F. G.; Harms, K.; Li, X. Y. *Inorg. Chem. Commun.* **2013**, *30*, 139–142.
- (14) (a) Li, X. Y.; Yu, F. L.; Sun, H. J.; Huang, L. Y.; Hou, H. Q. *Eur. J. Inorg. Chem.* **2006**, *2006*, 4362–4367. (b) Zhao, H.; Li, X. Y.; Zhang, S. M.; Sun, H. J. *Z. Anorg. Allg. Chem.* **2015**, *641*, 2435–2439.
- (15) (a) Matsubara, K.; Sueyasu, T.; Esaki, M.; Kumamoto, A.; Nagao, S.; Yamamoto, H.; Koga, Y.; Kawata, S.; Matsumoto, T. *Eur. J. Inorg. Chem.* **2012**, *2012*, 3079–3086. (b) Przyjowski, J. A.; Arman, H. D.; Tonzetich, Z. J. *Organometallics* **2013**, *32*, 723–732.
- (16) (a) Dai, W.; Xiao, J.; Jin, G.; Wu, J.; Cao, S. J. *Org. Chem.* **2014**, *79*, 10537–10546. (b) Schaub, T.; Fischer, P.; Steffen, A.; Braun, T.; Radius, U.; Mix, A. J. *J. Am. Chem. Soc.* **2008**, *130*, 9304–9317.
- (17) Karsch, H. H. *Chem. Ber.* **1977**, *110*, 2699–2711.
- (18) Klein, H. F.; Karsch, H. H. *Chem. Ber.* **1975**, *108*, 944–955.
- (19) Klein, H. F.; Karsch, H. H. *Angew. Chem., Int. Ed. Engl.* **1971**, *10*, 343–344.
- (20) (a) Bollmann, A.; Blann, K.; Dixon, J. T.; Hess, F. M.; Killian, E.; Maumela, H.; McGuinness, D. S.; Morgan, D. H.; Neveling, A.; Otto, S.; Overett, M.; Slawin, A. M. Z.; Wasserscheid, P.; Kuhlmann, S. J. *J. Am. Chem. Soc.* **2004**, *126*, 14712–14713. (b) Organ, M. G.; Abdel-Hadi, M.; Avola, S.; Hadei, N.; Nasielski, J.; O'Brien, C. J.; Valente, C. *Chem. - Eur. J.* **2007**, *13*, 150–157.